9664 *Inorg. Chem.* **2010**, *49*, 9664–9670
DOI: 10.1021/ic1014048

Inorganic Chemistry
Article

Synthesis and Crystal Structure from X-ray Powder Diffraction Data of Two Zirconium Diphosphonates Containing Piperazine Groups

Marco Taddei,* Ferdinando Costantino, and Riccardo Vivani

Department of Chemistry, University of Perugia, Via Elce di Sotto 8, 06123 Perugia, Italy

Received July 14, 2010

Two new zirconium aminophosphonates have been obtained by reaction of Zr(IV) with piperazine-*N,N′*-bis-(methylenephosphonate) building blocks. Their crystal structure has been determined ab initio from X-ray powder diffraction data collected with a conventional diffractometer. Although prepared in similar conditions, their composition and crystal structure is markedly different. Compound **1**, of formula $Zr_2H_4[(O_3PCH_2)_2N_2C_4H_8]_3 \cdot 9H_2O$, has a three-dimensional structure (trigonal, space group $R\bar{3}$ (No. 148), $a = 19.9400(9)$ Å, $c = 9.5728(6)$ Å, $Z = 3$), made of infinite inorganic chains of ZrO_6 octahedra and PO_3C tetrahedra, running along the *c*-axis direction, connected by piperazine groups in the *ab* plane, and generating channels running along the *c* axis. Compound **2**, of formula $ZrF_2(O_3PCH_2)_2(NH)_2C_4H_8$, has a pillared-layered structure (monoclinic, space group $P2_1/c$ (No. 14), $a = 8.7148(2)$ Å, $b = 8.1731(1)$ Å, $c = 9.0134(2)$ Å, $\beta = 105.175(1)°$ $Z = 2$) in which inorganic layers, made of the connectivity of Zr octahedra and P tetrahedra, are covalently connected by piperazine groups, that act as pillars. The effect of the various synthesis parameters is discussed. A probable structure directing parameter seems to be the pH value of the starting precipitation solution, that can influence the protonation of N atoms of piperazine moiety.

Introduction

Coordination polymers are today a large class of materials of great academic and industrial interest, mainly because of their structural versatility, facile functionalization, and good thermal robustness.[1] Most of the recent work on this topic has been focused on the so-called metal organic frameworks (MOF), which are typically based on transition metals coordinated by polytopic O- or N-donor ligands, such as carboxylate or amino groups. Highly predictable frameworks, often showing spectacular porous structures, have been recently obtained.[2]

Metal phosphonates (MP) can be considered as an alternative to traditional MOF. They generally offer a chemically and thermally robust framework and are characterized by a vast structural variety. This is mainly due to the fact that $R-PO_3$ phosphonate groups can behave as mono-, bi-, or tridentate, mono- or dianionic ligands. As a result of this, the structure of MP is still poorly predictable, especially when polyphosphonate building blocks are used, notwithstanding the intense research activity on this topic in the past decade.[3] This peculiarity, on one hand, can be considered a limit for the development of this class of materials; however, on the other hand, it may be seen as a precious source of new structural archetypes, potentially useful for diverse applications. In recent years, aminophosphonate building blocks have been widely employed, probably because of their relatively easy synthesis and their ability to induce the formation of highly ordered structures, owing to the presence of strongly polar amino groups that may act as structure directing agents. Several interesting transition metal and lanthanide aminomethylenephosphonates, bearing various functional organic groups, and sometimes with a porous open framework architecture, have been recently obtained.[4]

Zirconium aminophosphonates are very insoluble and stable compounds. From a structural point of view, they

*To whom correspondence should be addressed. E-mail: marcotaddei@hotmail.com.

(1) (a) Robin, A. Y.; Fromm, K. M. *Coord. Chem. Rev.* **2006**, *250*, 2127–2157. (b) Cheetham, K.; Rao, C. N. R.; Feller, R. K. *Chem. Commun.* **2006**, 4780–4795. (c) Janiak, C. *J. Chem. Soc., Dalton Trans.* **2003**, 2781–2804. (d) Rao, C. N. R.; Cheetham, K.; Thirumurugan *J. Phys.: Condens. Matter* **2008**, *20*, 083202.

(2) (a) Mellot-Draznieks, C.; Dutour, J.; Férey, G. *Angew. Chem.* **2004**, *116*, 6450–6456. (b) Ferey, G.; Mellot-Draznieks, C.; Serre, C.; Millange, F.; Dutour, J.; Surblè, S.; Margiolaki, I. *Science* **2005**, *309*, 2040–2042. (c) Deng, H.; Olson, M. A.; Stoddart, J. F.; Yaghi, O. M. *Nature Chem.* **2010**, *2*, 439–443. (d) Long, J. R.; Yaghi, O. M. *Chem. Soc. Rev.* **2009**, *38*, 1213–1214. (e) Bureekaew, S.; Shimomura, S.; Kitagawa, S. *Sci. Technol. Adv. Mater.* **2008**, *9*, 014108.

(3) (a) Poojary, D. M.; Hu, H.-L.; Campbell, F. L., III; Clearfield, A. *Acta Crystallogr.* **1993**, *B49*, 996–1001. (b) Clearfield, A. In *Prog. Inorg. Chem.*; Karlin, K. D., Ed.; John Wiley & Sons: New York, 1998; Vol. *47*, pp 374−510. (c) Alberti, G. In *Comprehensive Supramolecular Chemistry*; Alberti, G., Bein, T., Eds., Pergamon Press: Oxford, 1996; Vol. *7*, Chapter 5. (d) Clearfield, A.; Costantino, U. In *Comprehensive Supramolecular Chemistry*; Alberti, G., Bein, T., Eds., Pergamon Press: Oxford, 1996; Vol. *7*, Chapter 4. (e) Kong, D.; Li, Y.; Ouyang, X.; Prosvirin, A. V.; Zhao, H.; Ross, J. H., Jr.; Dunbar, K. R.; Clearfield, A. *Chem. Mater.* **2004**, *16*, 3020–3031. (f) Maeda, K. *Microporous Mesoporous Mater.* **2004**, *73*, 47–55.

(4) (a) Stock, N.; Rauscher, M.; Bein, T. *J. Solid State Chem.* **2004**, *177*, 642–647. (b) Du, Z.-Y.; Xu, H.-B.; Mao, J.-G. *Inorg. Chem.* **2006**, *45*, 9780–9788. (c) Mao, J.-G. *Coord. Chem. Rev.* **2007**, *251*, 1493–1520.

 Published on Web 09/23/2010 © 2010 American Chemical Society

feature a good regularity of metal environment geometry, which is strictly octahedral.[5] When they contain similar aminophosphonate building blocks, they often show the same architecture and connectivity of the inorganic backbone. For example, the class of Zr R-amino-*N*,*N*-bis(methylenephosphonates), with R = pentyl, butanoic, and benzyl group, has similar connectivity.[5,6] However, this is not a rule: for example, Zr tetraphosphonates containing $(O_3PCH_2)_2N$-R-$N(CH_2PO_3)_2$ building blocks feature very different structures when R is a butyl or a cyclohexyl group.[7] Different architectures have been previously found with other aminophosphonate building blocks.[8]

Recent literature presented piperazine-*N*,*N*′-bis(methylenephosphonate) as an intriguing building block, able to generate different open framework structures with several cations: Mn, Co, Ni, and Cu;[9] Ti and Al;[10] or lanthanides (La, Ce, and Nd).[11] Some of them show permanent porosity, while others possess a flexible open framework structure. Also, for these compounds, although very interesting from both a fundamental and practical point of view, a rational structural prediction has not been formulated yet.

This paper reports the preparation and characterization of two Zr derivatives of piperazine-*N*,*N*′-bis(methylenephosphonate), showing very different structures and compositions. One of them has a compact pillared layered structure, while the other shows a 3D framework architecture featuring infinite channels able to reversibly adsorb and desorb water.

Experimental Section

Chemicals. $ZrOCl_2 \cdot 8H_2O$ was a Merck Pro Analysi product. All of the other chemicals were Carlo Erba RPE grade. All reagents were used as received without further purification.

Synthesis of the Diphosphonic Acid. Piperazine-*N*,*N*′-bis(methylenephosphonic acid) $(H_2O_3PCH_2)_2N_2C_4H_8$ (hereafter H_4L) was prepared according to the Moedritzer Irani method[12] and purified by reprecipitation in tetrahydrofuran (THF; yield: 80%).

The solid was then characterized by the determination of its melting point; C, H, and N elemental analysis; and X-ray powder diffraction qualitative phase analysis. The molecular structure was checked with ^1H and ^{31}P liquid NMR.

Synthesis of $Zr_2H_4[(O_3PCH_2)_2N_2C_4H_8]_3 \cdot 9H_2O$ (1). A mixture of 1.5 mmol of H_4L dissolved in 15 mL of water and 4.5 mL of NH_3, 1 M, was added to a solution of 1 mmol of $ZrOCl_2 \cdot 8H_2O$ and 6 mmol of NH_4F in 10 mL of water. The starting pH value was about 7. The closed plastic vessel was then put in an oven at 80 °C for 6 days.The white solid formed was filtered and washed with NH_3, 0.1 M, and dried at 70 °C. Yield: 270 mg, 47% (calculated on Zr). Elemental analysis calcd (found) Zr: 15.75 (15.53); P: 16.06 (16.23); N: 7.25 (6.87); C: 18.65 (17.56); H: 5.01 (4.91).

Synthesis of $ZrF_2(O_3PCH_2)_2(NH)_2C_4H_8$ (2). A mixture of 1 mmol of H_4L in 20 mL of water and 2.5 mL of NH_3, 1 M, was added to a solution containing 1 mmol of $ZrOCl_2 \cdot 8H_2O$ and 2.1 mL of HF 2.9 M (6 mmol) in a plastic vessel. The starting pH value was about 2. The closed vessel was then put in an oven at 80 °C for 6 days. The white solid formed was filtered, washed with NH_3, 0.1 M, and dried at 70 °C. Yield: 200 mg, 50% (calculated on Zr). Elemental analysis calcd (found) Zr: 22.74 (22.68); P: 15.45 (15.21); F: 9.47 (9.65); N: 6.98 (6.77); C: 17.95 (18.15); H: 3.49 (3.57).

Analytical Procedures. X-ray powder diffraction (XRPD) patterns for structure determination and Rietveld refinements were collected according to the step scanning procedure with the Cu Kα radiation on a PANalytical X′PERT PRO diffractometer, PW3050 goniometer equipped with an X′Celerator detector. The LFF ceramic tube was operated at 40 KV, 40 mA. To minimize preferred orientations, the samples were carefully side-loaded onto an aluminum sample holder with an orientated quartz monocrystal underneath. Temperature-dependent X-ray diffraction (TDXD) patterns were collected in the 6−70° 2θ range with a powder diffractometer combining the curved position-sensitive detector (CPS120) from INEL and a high temperature attachment developed by Rigaku with a heating rate of 7 °C h^{-1}, in the 25−150 °C range. The counting time was 45 min for each diffraction pattern. The detector was used in a semifocusing geometry by reflection with the monochromatic Cu $K\alpha_1$ radiation, as described elsewhere.[13] Thermogravimetric (TG) measurements were performed using a Netzsch STA490C thermoanalyzer under a 20 mL min^{-1} air flux with a heating rate of 5 °C min^{-1}. Zr and P content of samples was obtained by ICP optical emission spectrophotometry using a Varian Liberty Series II instrument working in axial geometry. Fluorine content was determined as fluoride by ion chromatography: about 0.1 g of sample was refluxed for 3 h with 10 mL of 1 M NaOH up to complete hydrolysis. The resulting solution was filtered, properly diluted, and analyzed with a Dionex series 2000 i/sp instrument, using an IonPack AS4A column and a buffer solution, with the following composition: 1.7×10^{-3} M in $NaHCO_3$ and 3.5×10^{-3} M in Na_2CO_3 as eluent. C, N, and H contents were determined by elemental analysis using an EA 1108 CHN Fisons instrument. FT-IR spectra of the solid samples were recorded in transmittance mode under vacuum with a Bruker IFS 113 V spectrophotometer by the KBr pellet technique.

Structure Determination and Refinement for 1 and 2. Crystal structures were solved ab initio from X-ray powder diffraction data. The diffraction patterns were fitted and decomposed into the $K\alpha_1$ and $K\alpha_2$ contributions using a Pearson VII profile function, and the positions of the first 20 $K\alpha_1$ maxima were accurately determined for the indexing procedures. Indexing was performed using both the TREOR[14] and the DICVOL06[15] programs. The refined unit cell parameters are shown in Table 1. Space groups were assigned on the basis of a systematic comparison of the number of peaks found and the number of possible peaks, within all space groups of the respective crystal symmetry, using the Chekcell program.[16]

Structural models of **1** and **2** were determined using the real space global optimization methods implemented in the FOX program.[17] This software optimizes a structural model described by the use of building blocks defined in terms of their internal coordinates, such

(5) Vivani, R.; Alberti, G.; Costantino, F.; Nocchetti, M. *Microporous Mesoporous Mater.* **2008**, *107*, 58–70.
(6) (a) Costantino, U.; Nocchetti, M.; Vivani, R. *J. Am. Chem. Soc.* **2002**, *124*, 8428–8434. (b) Vivani, R.; Costantino, U.; Nocchetti, M. *J. Mater. Chem.* **2002**, *12*, 3254–3260.
(7) Vivani, R.; Costantino, F.; Costantino, U.; Nocchetti, M. *Inorg. Chem.* **2006**, *45*, 2388–2390.
(8) (a) Poojary, D. M.; Zhang, B.; Clearfield, A. *J. Chem. Soc., Dalton Trans.* **1994**, 2453–2456. (b) Poojary, D. M.; Vermeulen, L. A.; Vicenzi, E.; Clearfield, A.; Thompson, M. E. *Chem. Mater.* **1994**, *6*, 1845–1849. (c) Vermeulen, L. A.; Fateen, R. Z.; Robinson, P. D. *Inorg. Chem.* **2002**, *41*, 2310–2312.
(9) (a) Groves, J. A.; Miller, S. R.; Warrender, S. J.; Mellot-Draznieks, C.; Lightfoot, P.; Wright, P. A. *Chem. Commun.* **2006**, 3305–3307. (b) Miller, S. R.; Pearce, G. M.; Wright, P. A.; Bonino, F.; Chavan, S.; Bordiga, S.; Margiolaki, I.; Guillou, N.; Férey, G.; Bourrelly, S.; Llewellyn, P. L. *J. Am. Chem. Soc.* **2008**, *130*, 15967–15981.
(10) Serre, C.; Groves, J. A.; Lightfoot, P.; Slawin, A. M. Z.; Wright, P. A.; Stock, N.; Bein, T.; Haouas, M.; Taulelle, F.; Férey, G. *Chem. Mater.* **2006**, *18*, 1451–1457.
(11) (a) Mowat, J. P. S.; Groves, J. A.; Wharmby, M. T.; Miller, S. R.; Li, Y.; Lightfoot, P.; Wright, P. A. *J. Solid State Chem.* **2009**, *182*, 2769–2778. (b) Groves, J. A.; Lightfoot, P.; Wright, P. A. *Inorg. Chem.* **2005**, *44*, 1736–1739.
(12) Moedritzer, K.; Irani, R. R. *J. Org. Chem.* **1966**, *31*, 1603–1607.
(13) Plevert, J.; Auffredic, J.-P.; Louer, M.; Louer, D. *J. Mater. Sci.* **1989**, *24*, 1913–1918.
(14) Werner, P. E.; Eriksson, L.; Westdhal, M. *J. Appl. Crystallogr.* **1985**, *18*, 367–370.
(15) Boultif, A.; Louer, D. *J. Appl. Crystallogr.* **2004**, *37*, 724–731.
(16) Laugier, J.; Bochu, B. *LMGP-Suite*; ENSP/Laboratoire des Materiaux et du Genie Physique: 38042 Saint Martin d'Heres, France, 2002.
(17) Favre-Nicolin, V.; Cerny, R. *J. Appl. Crystallogr.* **2002**, *35*, 734–743.

Table 1. Crystallographic Data and Refinement Details for **1** and **2**

compound	**1**	**2**
empirical formula	$C_{18}H_{58}N_6O_{27}P_6Zr_2$	$C_6H_{14}N_2O_6F_2P_2Zr$
formula weight	1158.5	401.2
crystal system	trigonal	monoclinic
space group	$R\bar{3}$	$P2_1/c$
a/Å	19.9400(9)	8.7148(2)
b/Å		8.1731(1)
c/Å	9.5728(6)	9.0134 (2)
β/deg		105.175(1)
V/Å^3	3296.2(3)	619.61(2)
Z	3	2
calcd density/g·cm^{-3}	1.75	2.15
wavelength/Å	1.5418	1.5418
pattern range, 2θ/deg	5−100	8−135
step scan increment, 2θ/deg	0.02	0.02
time per step/s	60	60
no. of data points	4750	6350
no. of reflections	1500	2243
no. of parameters	63	58
no. of restraints	29	0
R_p[a]	0.033	0.065
R_{wp}[b]	0.044	0.085
R_F2[c]	0.046	0.066
GOF[d]	4.0	2.9

[a] $R_p = \Sigma|I_o - I_c|/\Sigma I_o$. [b] $R_{wp} = [\Sigma w(I_o - I_c)^2/\Sigma w I_o^2]^{1/2}$. [c] $R_F2 = \Sigma|F_o^2 - F_c^2|/\Sigma|F_o^2|$. [d] GOF $= [\Sigma w(I_o - I_c)^2/(N_o - N_{var})]^{1/2}$.

as bond lengths, bond angles, and dihedral angles. Optimization was performed by comparing the XRPD patterns calculated from randomly generated configurations and using the "integrated *R*wp" (i*R*wp) as the cost function. Trial structures were generated using the "Parallel Tempering" algorithm.[18] The starting model was composed of the free metal atom and the organophosphonic group. Hydrogen atoms were omitted. Starting values for bond lengths and angles were taken from similar systems found in the literature and constrained within a standard deviation of 0.15 Å and 10°, respectively. All other dihedral angles were left to change freely. Antibump restraints (Zr−P distance = 3.0(5) Å) between the metal and the phosphorus atoms were applied in order to speed up the optimization process. Rietveld refinements of the structural models were performed using the GSAS program.[19] First, cell, sample displacement, background, and profile shape parameters were refined. A corrected pseudo Voigt profile function[20] (six terms) with two terms for the correction of asymmetry at the low-angle region was used. Then, atomic coordinates and isotropic displacement parameters were refined, restraining the distances to the following values: Zr−O = 2.00(5) Å, Zr−F = 1.95(5) Å, P−O = 1.55(5) Å, C−C = 1.54(5) Å, and C−N = 1.45(5) Å. The statistical weight of these restraints was decreased as the refinement proceeded, but for **1**, it was not possible to set it to zero, due to some unrealistic light atom bond distances. The atomic displacement parameters of the heavy atoms (Zr and P) were refined independently, while those of the light atoms (F, O, N, and C) were refined by constraining the program to apply the same shifts. Hydrogen atoms were not included in the refinement procedure. At the end of the refinement, the shifts in all parameters were less than their standard deviations. Table 1 lists the crystal data and refinement details, and Figure 1 shows the final Rietveld and difference plots.

Results

Description of the Structures. Compound **1** (Figure 2) has a three-dimensional structure, made of infinite inorganic chains of ZrO_6 octahedra and PO_3C tetrahedra, running

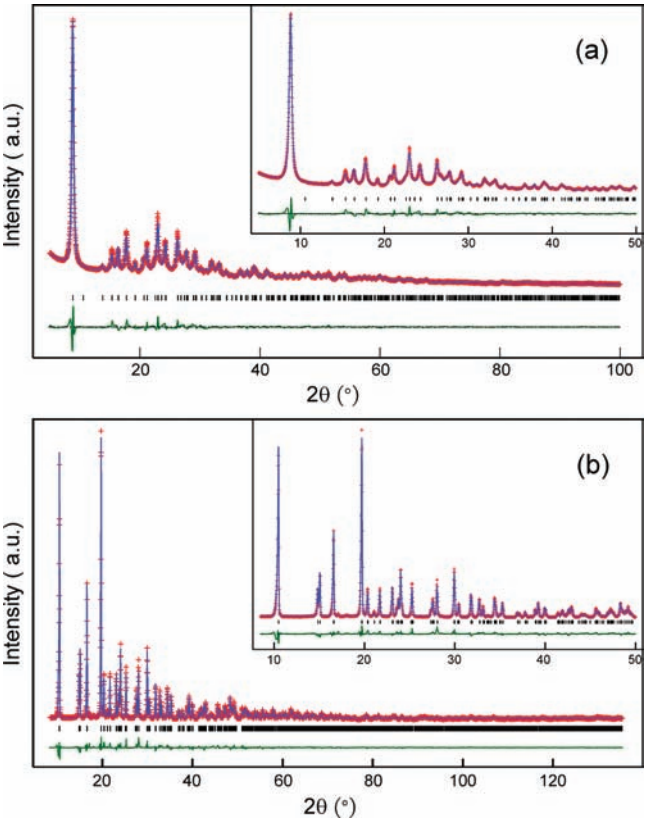

Figure 1. Final Rietveld plots for **1** and **2**, reporting the observed pattern (red symbols), the calculated pattern (blue line), and their difference (green line). Black markers at the bottom indicate the calculated positions of peaks.

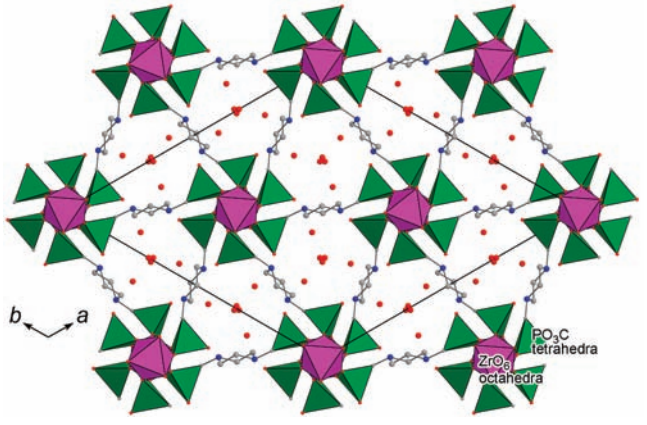

Figure 2. Polyhedral representation of the structure of **1**, viewed along the *c* axis.

along the *c*-axis direction, connected by piperazine groups in the *ab* plane. Each polymeric chain is built by the propagation along the *c*-axis, of "composite building units" (CBUs) formed by one Zr octahedron and three P tetrahedra (Figure 3). A similar polyhedra connectivity of the inorganic polymeric backbone was previously observed in a 1D Zr phosphate of formula $[enH_2][Zr(HPO_4)_3]$.[21]

Zr atoms lie in 3-fold inversion axes. Zr octahedra are bonded to six oxygen atoms belonging to six different phosphonates, and phosphonate tetrahedra act as exobidentate

(18) Falcioni, M.; Deem, M. W. *J. Chem. Phys.* **1999**, *110*, 1754–1767.
(19) Larson, C.; von Dreele, R. B. *Generalized Crystal Structure Analysis System*; Los Alamos National Laboratory: Los Alamos, NM, 2001.
(20) (a) Thompson, P.; Cox, D. E.; Hastings, J. B. *J. Appl. Crystallogr.* **1987**, *20*, 79–83. (b) Finger, L. W.; Cox, D. E.; Jephcoat, A. P. *J. Appl. Crystallogr.* **1994**, *27*, 892–900.
(21) Sung, H. H-Y.; Yu, J.; Williams, I. D. *J. Solid State Chem.* **1998**, *140*, 46–55.

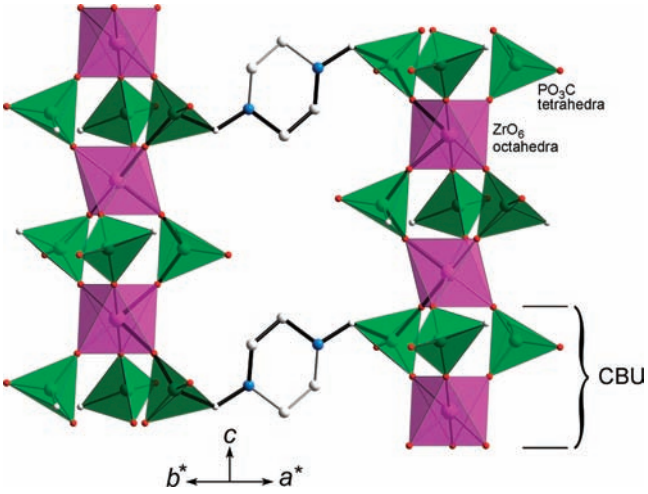

Figure 3. Portion of the structure of **1**, viewed along the [110] axis, showing the inorganic chains originated by the propagation of the indicated CBU. Bonds in bold show the 30-membered ring window between the adjacent channels running along the *c* axis.

groups, as they share two corners with two different Zr octahedra belonging to the same inorganic chain. The two other phosphonate corners are occupied by the organic group and a terminal P−O group. For the electroneutrality requirement, four of the six terminal P−O groups per formula unit should be protonated, while the remaining two must be P═O groups. Since all phosphorus and oxygen atoms involved in this bond (P1 and O2) are crystallographically equivalent, we may assume that the four hydrogen atoms are scrambled over the six P−O groups. Inorganic chains are packed in a 11.45 Å sided hexagonal pattern and form quasicylindrical channels centered on the 3-fold inversion axes, with 6.7 Å diameter from O2 to C2 (symmetry code: $0.66667 + x - y$, $0.33333 + x$, $0.33333 - z$) atomic centers. However, the free diameter reduces to about 3.2 Å when methylene and OH van der Waals radii are subtracted. The walls of these channels are formed by the piperazine groups arranged in a helicoidal fashion along the channels. Adjacent channels are separated by 30-membered ring windows of about 6.5 × 4.5 Å dimensions, from atomic centers (Figure 3).

Nine water molecules per formula unit are placed in the channels and interact with an intricated network of hydrogen bonds with the terminal P−OH/P═O groups. A series of difference Fourier maps allowed us to find two different sites, in general positions, each of them with a site multiplicity equal to 18, in the asymmetric unit. Since the full occupation of these sites should generate 12 water molecules per formula unit, during the Rietveld refinement, the sum of occupation factors of the two water sites was constrained to be 1.5, in order to fit the TG data (see later). After refinement, occupation factors of the two sites were found to be similar (0.78(1) and 0.72(1)).

Different from other Zr aminophosphonates, including compound **2**, nitrogen atoms of the amino groups do not directly interact with the free P−OH groups. Accordingly, FT-IR spectra seem to confirm that nitrogen atoms are unprotonated because the large band in the region 2600−2200 cm^{-1}, typical of the R_3N-H^+ stretching vibrations,[22] is absent (see Figure 10).

Titration experiments of **1** with NaOH or LiOH solutions showed that the free P−OH groups did not possess appreciable ion exchange capacity toward Na^+ or Li^+, probably because of an hindered diffusion through the channels.

Compound **2** has a pillared-layered structure in which inorganic layers, made of the connectivity of Zr octahedra and P tetrahedra, and lying on the [100] crystallographic planes, are covalently connected by piperazine groups, that act as pillars (Figure 4).

Every Zr atom is placed in the [100] plane. Each of them is trans-coordinated by two fluorine atoms. The octahedron axis defined by the F−Zr−F bond sequence is tilted, alternatively on one side and the other, about 30° to the layer plane, both on *b* and *c* directions. The four equatorial positions are occupied by four oxygen atoms belonging to four different phosphonate tetrahedra. They share two corners with two different Zr octahedra belonging to the same inorganic plane. This connectivity creates a quasi-square pattern based on 16-atom (eight polyhedra) rings, that constitute the inorganic planes (Figure 5).

The remaining P−O group not coordinated to the metal atom is directed toward the nitrogen atom of the piperazine moiety belonging to the nearest adjacent phosphonate group. The PO···N distance is 2.74 Å, indicating that a hydrogen bond is present between the two atoms. This kind of interaction obviously occurs also on the other nitrogen atom at the opposite side of piperazine moiety, which is crystallographically equivalent. Therefore, all nitrogen atoms are involved in H bonds with P−O groups. We cannot assess if the piperazine group is protonated, because we were not able to detect the position of the hydrogen between N and O atoms by our diffraction data. However, several papers reporting single crystal X-ray structural data on similar metal piperazine bis(methylenephosphonate),[9a,10,11] show that, when the nitrogen atoms are involved in hydrogen bonds with free P−O groups, they are protonated. Therefore, we have assumed that in **2** both nitrogen atoms of piperazine groups are protonated. The presence in the IR absorption spectrum of several superimposed bands of medium intensity in the range 2600−2200 cm^{-1}, which can be referred to the R_3N-H^+ vibrations,[22] supports this assumption (see Figure 10).

Piperazine groups occupy the interlayer domain in a close packed herringbone arrangement. The free area associated to each piperazine group (36.8 $Å^2$, $b \times c/2$) is almost completely filled, as shown in Figure 6, because the piperazine longitudinal axis is tilted about 38° toward the *c* direction, from the perpendicular of the inorganic layers. Fluorine atoms do not engage any noncovalent strong interaction with other atoms.

Thermal Behavior. TG curves for **1** and **2** are shown in Figure 7. **1** starts to lose water at about 50 °C and is completely dehydrated at 150 °C. Weight loss at this temperature is 14.33%, in agreement with the loss of nine hydration water molecules per formula weight (calc 13.98%). This value was found to be highly reproducible through a large set of samples, and therefore, the occupancy factors of water oxygen atoms were set accordingly during Rietveld refinements. Water loss is completely reversible, and the sample can fully rehydrate in some hours. TDXD shows that, during

(22) The band assignments have been made according to Socrates, G. *Infrared and Raman Characteristic Group Frequencies: Tables and Charts*; John Wiley & Sons: Chichester, 2001.

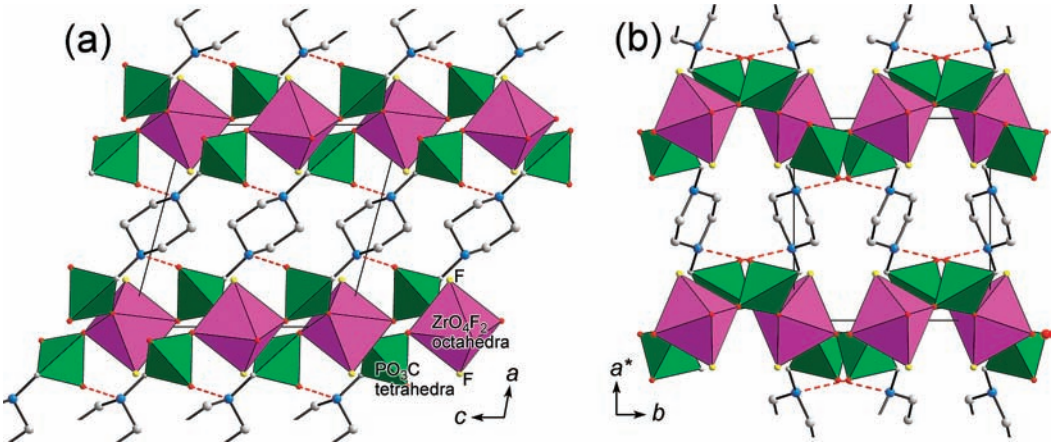

Figure 4. Polyhedral representation of the structure of **2**, viewed along the *b* axis (a) and *c* axis (b).

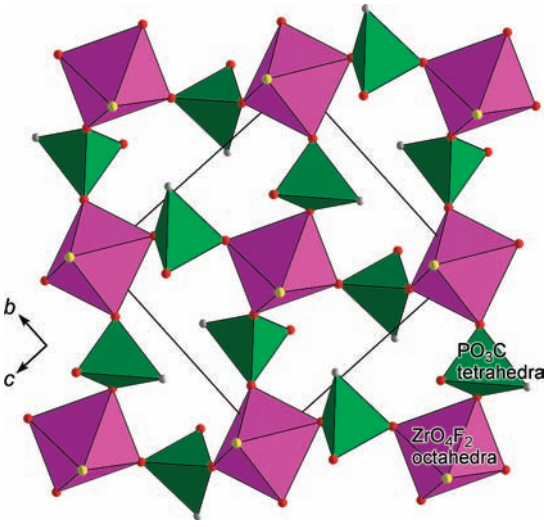

Figure 5. Polyhedral scheme of the inorganic layer of **2** made of the connectivity of ZrO_4F_2 octahedra and PO_3C tetrahedra.

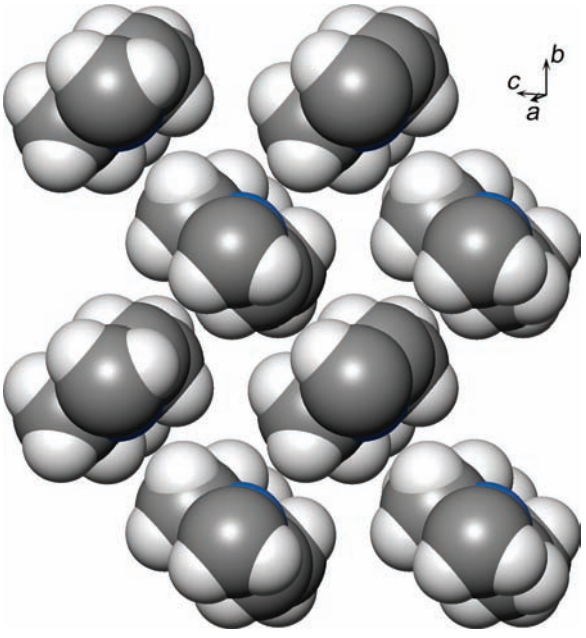

Figure 6. Scheme of the packing of piperazine groups of **2** viewed down the piperazine longitudinal axis, which is tilted approximately 38° from the perpendicular of the inorganic layers. Hydrogen atoms are added in their calculated positions, and all atoms are represented with their VdW average radii (C, 1.60 Å; H, 1.10 Å).

dehydration, the 110 reflection is gradually shifted toward higher 2θ values, the *d* value changing from 10.02 Å at room temperature to 9.02 Å at 150 °C (Figure 8). In addition, during heating, a gradual degradation of the whole pattern is observed. The pattern taken at 150 °C shows only some large bands, besides the shifted 110 reflection. In agreement with TG data, when cooling, the XRPD changes are fully reversible, and crystallinity is completely recovered (Figure 9).

Due to this behavior, refinement of the anhydrous structure, devoted to highlight the effect of dehydration on the framework, was not possible. However, it is likely that, owing to the partial flexibility of organic interlinking groups, the loss of water induces a structural contraction, mainly involving [110] planes, without any bond breaking, due to the collapse of empty channels.

As a consequence of its structural flexibility, **1** did not show appreciable microporosity by nitrogen adsorption measurements carried out at 77 K.

At about 300 °C, the TG curve shows a weight loss due to the decomposition of organics. At the end of TG analysis, at 1200 °C, only cubic ZrP_2O_7 was found; therefore, the weight loss at about 900 °C may be ascribed to the loss of the excess of phosphorus, as P_2O_5. The total weight loss

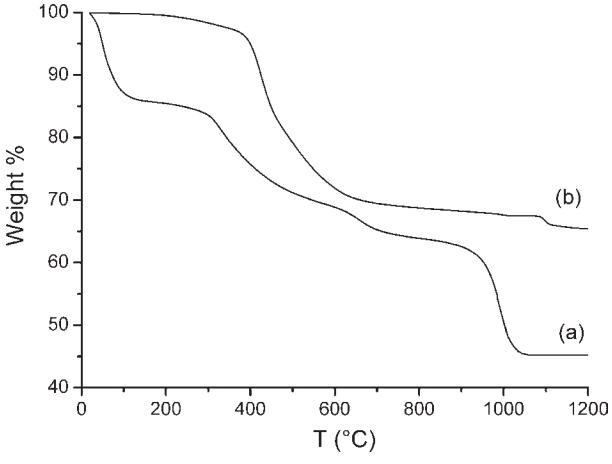

Figure 7. TG curves for **1** (a), and **2** (b).

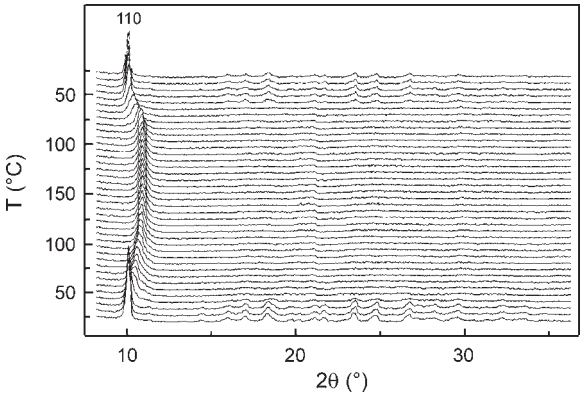

Figure 8. Study of the dehydration−hydration process of **1** using temperature-dependent X-ray diffractometry.

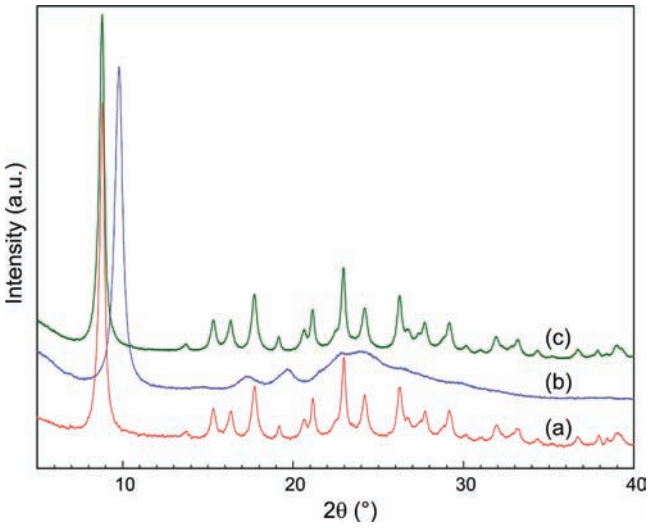

Figure 9. Comparison of XRPD patterns of **1** at room temperature (a), at 150 °C (b), and at room temperature after heating (c).

is 54.80%, in good agreement with the calculated value (54.21%).

Weight loss of **2** starts after about 200 °C and consists of a series of unresolved steps. At the end of TG analysis, at 1200 °C, only cubic ZrP_2O_7 was found. The total weight loss is 35.10%, in agreement with the calculated value (33.90%).

FT-IR Spectra. FT-IR spectra of **1** and **2** are reported in Figure 10.[22] A very large band attributed to the O−H stretching and bending vibration of interacting water and PO−H groups through H bonds can be clearly observed in **1** in the 3600−2800 cm^{-1} region. The same band is very weak in **2** and may be ascribed to a small amount of adsorbed water. The C−H stretching vibration bands of the organic group are very evident, especially for **2**, near 3000 cm^{-1}. The large band in the region 2600−2200 cm^{-1}, characteristic of the R_3N-H^+ stretching vibrations is absent in **1** and is very large in **2**, according to their structural features. The complex system of bands in the region 1500−400 cm^{-1} is due to the vibration of the rest of the framework, especially Zr−O, P−O, and P−C stretching modes.

Discussion

Although prepared in similar conditions, **1** and **2** have significantly different compositions and structures. Granted that correlation between the many synthesis parameters and

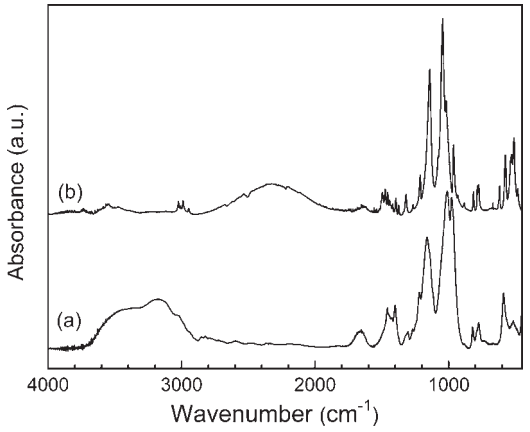

Figure 10. FT-IR spectra of **1** (a) and **2** (b).

the structural and chemical features of the obtained compounds is often difficult, some considerations can be attempted. For the synthesis procedures reported here, starting P/Zr molar ratios (R) in solution are equal to those in solid phases: 3 for **1** and 2 for **2**. However, our tests showed that the products obtained are not influenced by the R value in solution. For example, for **1**, when R in solution is set to 2, the system still prefers the formation of the same solid, with a higher R value than in solution, although with a lower yield. This should mean that R in solution is not a driving parameter. A similar consideration can be made for the F/Zr molar ratio (R′). In this kind of synthesis, fluoride ions are used to prevent a fast precipitation of the very insoluble Zr phosphonates, because they form soluble fluorocomplexes with Zr. By increasing the temperature, the stability of such complexes tends to decrease, and phosphonate groups can gradually replace fluorine atoms from the Zr coordination sphere, thus leading to a slow crystallization of the solid phase. In some cases, fluorine atoms can remain in the solid phase, coordinated to zirconium. For our systems, R′ in solution is the same (R′ = 6) for both procedures; on the contrary, R′ in the solid is lower for **1** (R′ = 0, fluorine is absent) than for **2** (R′ = 2). Therefore, also in this case, the mere F/Zr molar ratio in solution seems to be a nonrelevant parameter.

The main difference in the composition of starting solutions is the amount of ammonia/ammonium, which is 10.5 mol/mol of Zr for **1** and 2.5 for **2**. Due to this difference, the starting pH is markedly higher in **1** (pH about 7) than in **2** (pH about 2). The formation of the Zr derivative involves a series of intricate equilibria of acid−base and coordination type, and the effect of an important variable such as pH cannot be easily simplified. However, we report some observations that let us suppose that an important effect of pH may be the protonation level of nitrogen atoms of aminophosphonate groups and that this can be a real structure directing factor.

The presence of residual fluorine atoms coordinated to zirconium is often accompanied by the presence of protonated nitrogen atoms of the amino groups, that interact through hydrogen bonds with adjacent P−O groups. For example, several Zr monoaminodiphosphonates show one Zr−F bond and one PO···HN interaction/formula unit,[6] while in traditional all-carbon Zr phosphonates, fluorine is generally absent and Zr is fully coordinated to phosphonate groups in the usual α-layered structure.[3] In our case, **1**, which is obtained at a higher pH value, does not show both fluorine

atoms and protonated nitrogens, while **2**, which is obtained at lower pH value, shows two F atoms and two protonated amino groups/formula unit. Therefore, it seems that when the nitrogen atoms of aminophosphonate building blocks are protonated and, therefore, positively charged, anionic P−O groups tend to closely interact with them, in order to reduce local charge, and thus leave one or two zirconium coordination sites to fluorine. In conclusion, a higher starting pH value, associated with a larger fraction of unprotonated piperazine diphosphonate, may favor the formation of a solid phase free from fluorine (**1**), while a lower pH value and a larger fraction of positively charged building blocks, may induce the formation of a compound containing fluorine and many strong PO···HN interactions (**2**) in a close packed structure.

Conclusions

Two new zirconium derivatives of the same aminomethylenediphosphonic acid have been obtained as pure phases and characterized. Their structures have been solved ab initio from X-ray powder diffraction data. The protonation level of nitrogen atoms of the amino phosphonate groups, that is influenced by the precipitation pH, was identified to be a possible structure directing factor, also affecting the composition of the two phases.

Future investigation will be devoted to verify if these effects may be extended to similar systems, thus giving a contribution to better understand the connections between the start (the synthetic parameters and the molecular structure of ligands) and the goal (the global crystal structure) in the run for the discovery and the rational design of new compounds in metal phosphonate chemistry.

Acknowledgment. We acknowledge Thierry Bataille, University of Rennes, France, for the TDXD experiments. This work has been supported by MIUR−PRIN.

Supporting Information Available: Crystallographic data and CIF files for **1** and **2**. This material is available free of charge via the Internet at http://pubs.acs.org.